

Prediction of ice crystal size distribution during freezing of a pharmaceutical solution

Original

Prediction of ice crystal size distribution during freezing of a pharmaceutical solution / Arsiccio, Andrea; Barresi, Antonello; Pisano, Roberto. - ELETTRONICO. - (2017), pp. 1-8. (Intervento presentato al convegno EuroDrying'2017 – 6th European Drying Conference tenutosi a Liège, Belgium nel June 19-21, 2017).

Availability:

This version is available at: 11583/2683386 since: 2018-08-09T19:50:11Z

Publisher:

University of Liège

Published

DOI:

Terms of use:

This article is made available under terms and conditions as specified in the corresponding bibliographic description in the repository

Publisher copyright

(Article begins on next page)

PREDICTION OF ICE CRYSTAL SIZE DISTRIBUTION DURING FREEZING OF A PHARMACEUTICAL SOLUTION

A. Arsiccio, A. A. Barresi*, R. Pisano

Department of Applied Science and Technology, Politecnico di Torino

**E-mail of the corresponding author: antonello.barresi@polito.it*

Abstract: In this work, a mathematical model is presented for the prediction of the crystal size distribution of ice over the entire height of products frozen in vials. Unlike previous approaches, which were all based on empirical observations, the present one makes use of principles of chemistry and physics. In particular, we focus on a simplified version of such model and show its applicability to typical pharmaceutical formulations. The model predictions have been validated analyzing with Scanning Electron Microscopy the pore dimension of freeze-dried products, which corresponds to the ice crystal dimension of frozen products.

Keywords: freezing, crystal sizing, mathematical modeling, freeze-drying, pharmaceutical solutions

Introduction

Prediction of the crystal size of solvent in frozen products is a fundamental issue in several fields of technology. For example, the ice crystal dimension of products to be freeze-dried is a critical aspect [1, 2, 3, 4], as it is linked to the thermal stresses for the product as well as to the processing times [5]. Larger crystals, in fact, will result in a shorter primary drying, while secondary drying will be longer. Thus, an optimal dimension has to be found in order to improve the process as a whole. From this viewpoint, the possibility to predict ice crystal size would be extremely advantageous.

As a consequence of the importance of the subject, many research works have been developed to obtain a quantitative relationship that correlates the thermal history with the size of the ice crystals, but these are all empirical formulas and lack of physical explanation. Many of such works relate the ice crystal dimension, D_p , with the temperature gradients within the frozen zone θ and the freezing front velocity v [6, 7, 8]:

$$D_p = \alpha \theta^{-\lambda_1} v^{-\lambda_2} \quad (1)$$

Where α , λ_1 and λ_2 are adjustable coefficients that vary according to the type of product and process, covering a wide range and sometimes changing even within the same application, as shown in Table 1.

Table 1. Empirical laws for crystal sizing

Application	Correlation	Reference
Freezing of apples	$D_p \propto \theta^{-0.5} v^{-0.5}$	Bomben and King [6]
Alloy solidification at high rates	$D_p \propto \theta^{-0.5} v^{-0.25}$	Kochs at al. [7]
Metal solidification at low rates	$D_p \propto \theta^{-1} v^{-1}$ $D_p \propto v^{-0.5}$	Kurz and Fischer [8]

The aim of this work is the discussion of a mechanistic model capable of providing physical insight into the process and of predicting the ice crystal size distribution in wide ranges of conditions. The mathematical derivation explains from a physical point of view the previously assumed relation between D_p , v and θ . The model has been developed in both a detailed and a simplified version, but we will focus here on the simplified one. The simplified model is easier to implement, but it is valid for dilute solutions only. In spite of this limitation, it was able to predict with good accuracy the ice crystals dimension of typical pharmaceutical formulations. The validation was performed using SEM images of freeze-dried products, whose pore dimension corresponds to the ice crystal size of the frozen product.

Mathematical formulation

The domain under investigation is the cylinder of product, having height Δz and diameter D , where crystal growth is occurring. A picture of the domain under investigation is shown in Figure 1.

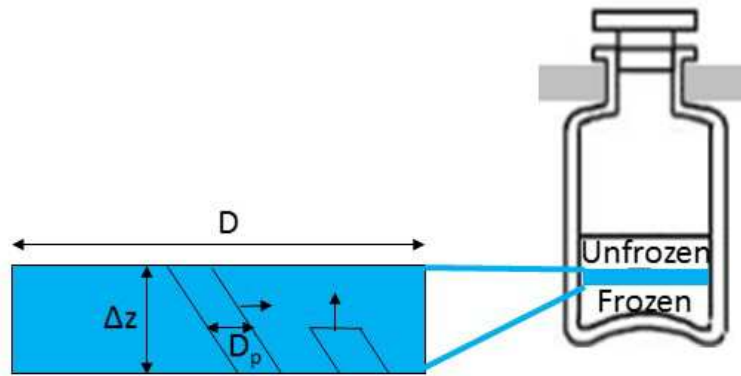


Fig. 1. Scheme of the domain under investigation.

In order to determine ice crystals size, an energy balance is written that describes the crystal growth process, once nucleation occurred. The domain considered changes its position during the process, as it follows the freezing front. Thus, the product height needs to be discretized into a finite number n of intervals, which will be denoted by subscript i .

During the process, the temperature of the freezing front and of the zone where freezing has not yet completed is almost constant and equal to the equilibrium value. Thus, it is reasonable to model our domain considering steady state conditions, as well as absence of energy exchange with the unfrozen zone. As a result, the following energy balance can be written:

$$\left(\begin{array}{c} \text{heat removal} \\ \text{by the} \\ \text{frozen product} \end{array} \right) + \left(\begin{array}{c} \text{heat transferred} \\ \text{from the} \\ \text{lateral surface} \end{array} \right) + \left(\begin{array}{c} \text{ice released} \\ \text{by ice} \\ \text{crystallization} \end{array} \right) + \left(\begin{array}{c} \text{enthalpy change} \\ \text{due to new} \\ \text{surface generation} \end{array} \right) = 0$$

$$-k_s \theta_i \pi \frac{D^2}{4} - \pi D \Delta z h \Delta T + \frac{dV_{ice,i}}{dt} \rho_{ice} \Delta H_f - \frac{dS_{ice,i}}{dt} \gamma = 0 \quad (2)$$

By approximating the derivatives with the corresponding finite increments, we get:

$$-k_s \theta_i \pi \frac{D^2}{4} - \pi D \Delta z h \Delta T + N_i \pi \frac{D_{p,i}^2}{4} \rho_{ice} v_i \Delta H_f - N_i \pi D_{p,i} v_i \gamma a_{s,i} = 0 \quad (3)$$

where $a_{s,i}$ is the ratio between the real ice surface area and the fictitious one calculated considering the ice crystals as perfect and smooth cylinders.

We can then combine the energy balance with the following mass balance:

$$\sum_{i=1}^n N_i \pi \frac{D_{p,i}^2}{4} \rho_{ice} \tau \Delta z = m \quad (4)$$

where m is the mass of water which crystallizes.

If we then assume that the mass of ice which crystallizes is proportional to the heat removed, we obtain the following equation:

$$D_{p,i} = \frac{16m\theta_i \gamma b v_i}{\rho_{ice} \theta_i^{\frac{2}{3}} (4m\theta_i v_i \Delta H_f - k_s \theta_i D^2 \pi \Delta z \sum_{i=1}^n \theta_i - 4\pi \Delta^2 z \sum_{i=1}^n [\theta_i D h \Delta T])} \quad (5)$$

where the term b accounts for surface irregularities and the real ice crystal habit.

This is the general result of the model.

However, we could assume that the solution is dilute, so that we can neglect heat transferred from the lateral surface. Moreover, we could write the following approximated mass balance:

$$\varepsilon \pi \frac{D^2}{4} \approx N_i \pi \frac{D_{p,i}^2}{4} \tau \quad (6)$$

where ε is the ratio between the volume of ice and the total volume of the system.

If we make these two approximations, we obtain a simpler equation:

$$D_{p,i} = \frac{4\varepsilon \gamma b v_i}{(\varepsilon \rho_{ice} v_i \Delta H_f - k_s \theta_i) \theta_i^{\frac{2}{3}}} \quad (7)$$

The product γb cannot be calculated theoretically and has therefore to be estimated by fitting of experimental data for crystal size vs product thickness. However, it has a physical meaning and was found to be independent of operating conditions, such as cooling rate and nucleation temperature.

We will focus here on the simplified model, Equation 7, which is easier to implement. We will show that it is valid for formulations and operating conditions which are typical of pharmaceutical processes.

Materials and Methods

The formulations investigated were mannitol or sucrose solutions. Mannitol and sucrose were purchased from Sigma Aldrich and used as supplied. The vials employed (type 1, 10R, 45x24 mm, Schott AG, Germany) were accurately filled with 3 ml of sample solution. A freeze-dryer LyoBeta 25 (Telstar, Terrassa, Spain) was used for the freeze-drying cycles. In order to monitor the temperature of the shelves and of the product a system of T-type copper/constantan miniature thermocouples was used.

The experiments were performed using the traditional shelf-ramped freezing technique. The vials were loaded onto the freeze-dryer shelves and then the refrigerating fluid temperature was decreased with a precise cooling rate until a value of -45°C was reached.

Table 2 lists the details of formulations and operating conditions investigated.

After freeze-drying, the pore dimension of the product obtained, which corresponds to the ice crystal size formed after freezing, was evaluated using SEM analysis (SEM, FEI type, Quanta Inspect 200, Eindhoven, the Netherlands). An example of SEM images is shown in Figure 2.

Table 2. Details of experimental tests

	Formulation	Cooling rate, K min⁻¹	Nucleation temperature, K
A	Mannitol 5% w/w	0.8	260.5
B	Sucrose 5% w/w	0.8	258.2
C	Mannitol 5% w/w	0.8	266.4
D	Mannitol 5% w/w	0.1	261.0
E	Mannitol 10% w/w	0.8	261.3

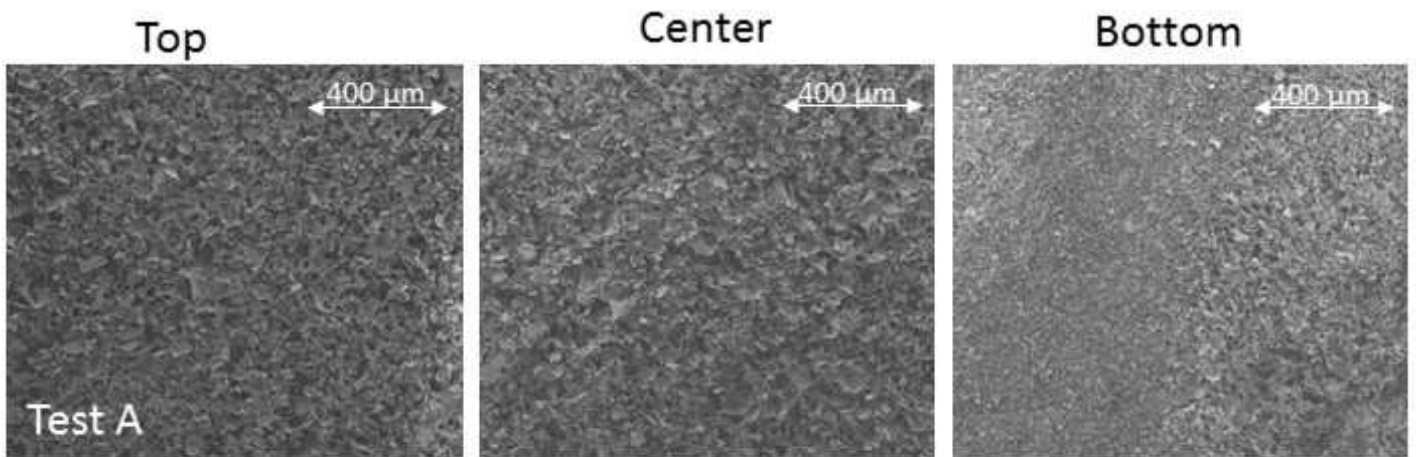


Fig. 2. SEM images at top, center and bottom of product for test E of Table 2.

The product temperature profiles during freezing were obtained using the model developed by Nakagawa et al. [9] and compared with the experimental value. The 2D axisymmetric model for temperature prediction was solved using the commercial software COMSOL Multiphysics. While the experimental measure provided the temperature value at a single point of the sample, Nakagawa's model allowed the estimation of temperature within the whole product. Thus, it provided the information required for the evaluation of v and θ , as described in Nakagawa et al. [9]. In fact, at the freezing front the temperature is equal to the equilibrium value and thus its position can be easily known; thus, v can be evaluated as the ratio between the variation of the freezing front position Δz_f and the time interval Δt :

$$v = \frac{\Delta z_f}{\Delta t} \quad (3)$$

Then, the temperature gradient θ is equal to the slope of the curve, at a given time, below the equilibrium freezing temperature.

An outline of the procedure employed is summarized in Figure 3.

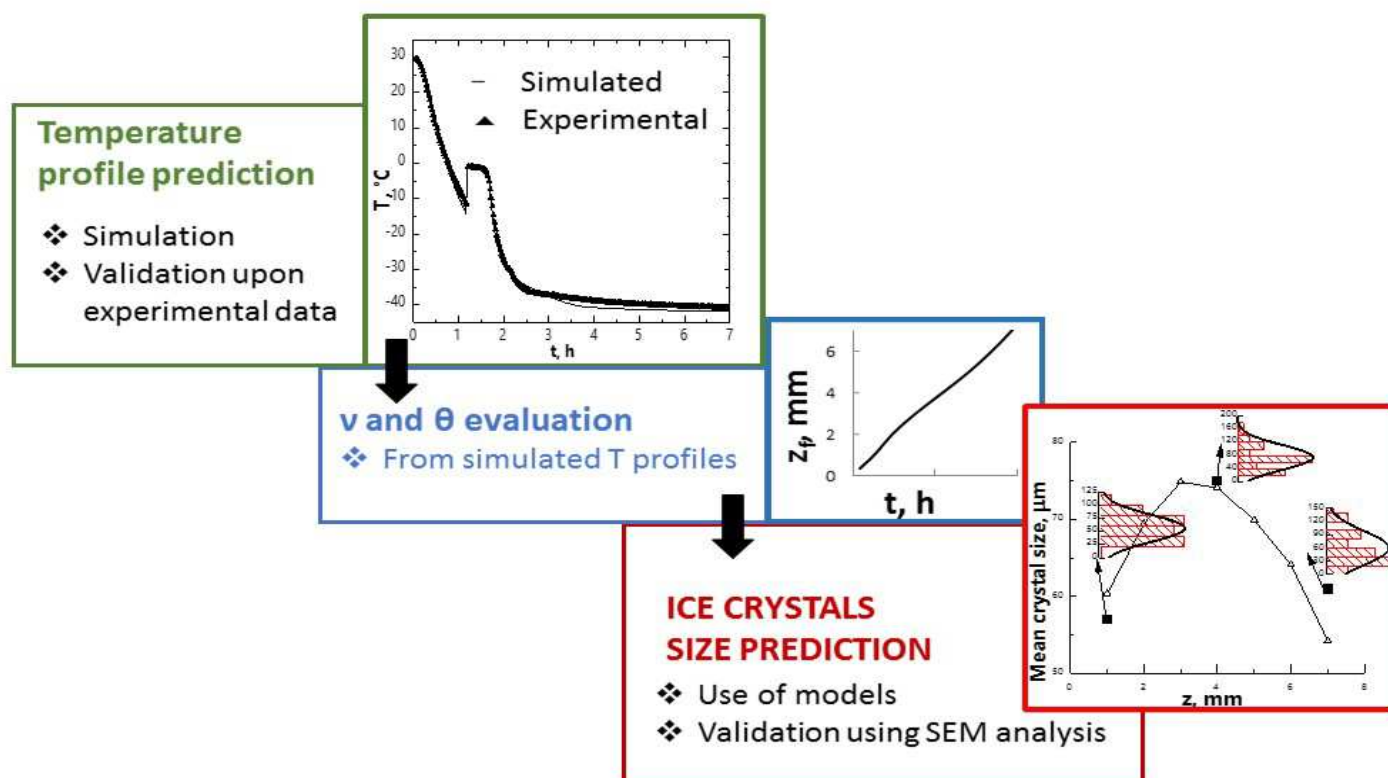


Fig. 3. Outline of the procedure employed to predict crystal size using temperature profiles.

Results and discussion

In this work we focused on the simplified model, Equation 7. The aim is to demonstrate its validity for formulations and operating conditions which are usually employed for pharmaceuticals.

The values of the parameters used in the model are listed in Table 3.

As can be seen from the Table, the numerical value of parameter γb is much higher for sucrose than for mannitol.

Table 3. Numerical values of the parameters employed

k_s	2.5	$\text{W m}^{-1} \text{K}^{-1}$
h	5	$\text{W m}^{-2} \text{K}^{-1}$
ρ_{ice}	918	kg m^{-3}
ΔH_f	333500	J kg^{-1}
γb (mannitol)	$7 \cdot 10^4$	$\text{J K}^{2/3} \text{m}^{-8/3}$
γb (sucrose)	$23 \cdot 10^4$	$\text{J K}^{2/3} \text{m}^{-8/3}$

The model for crystal sizing was validated using two different solutes, mannitol and sucrose, which represent an amorphous and a crystalline system respectively. Figure 4 shows that for both solutes, tests A and B, the model predicted fairly well the crystal size distribution as measured by SEM analysis.

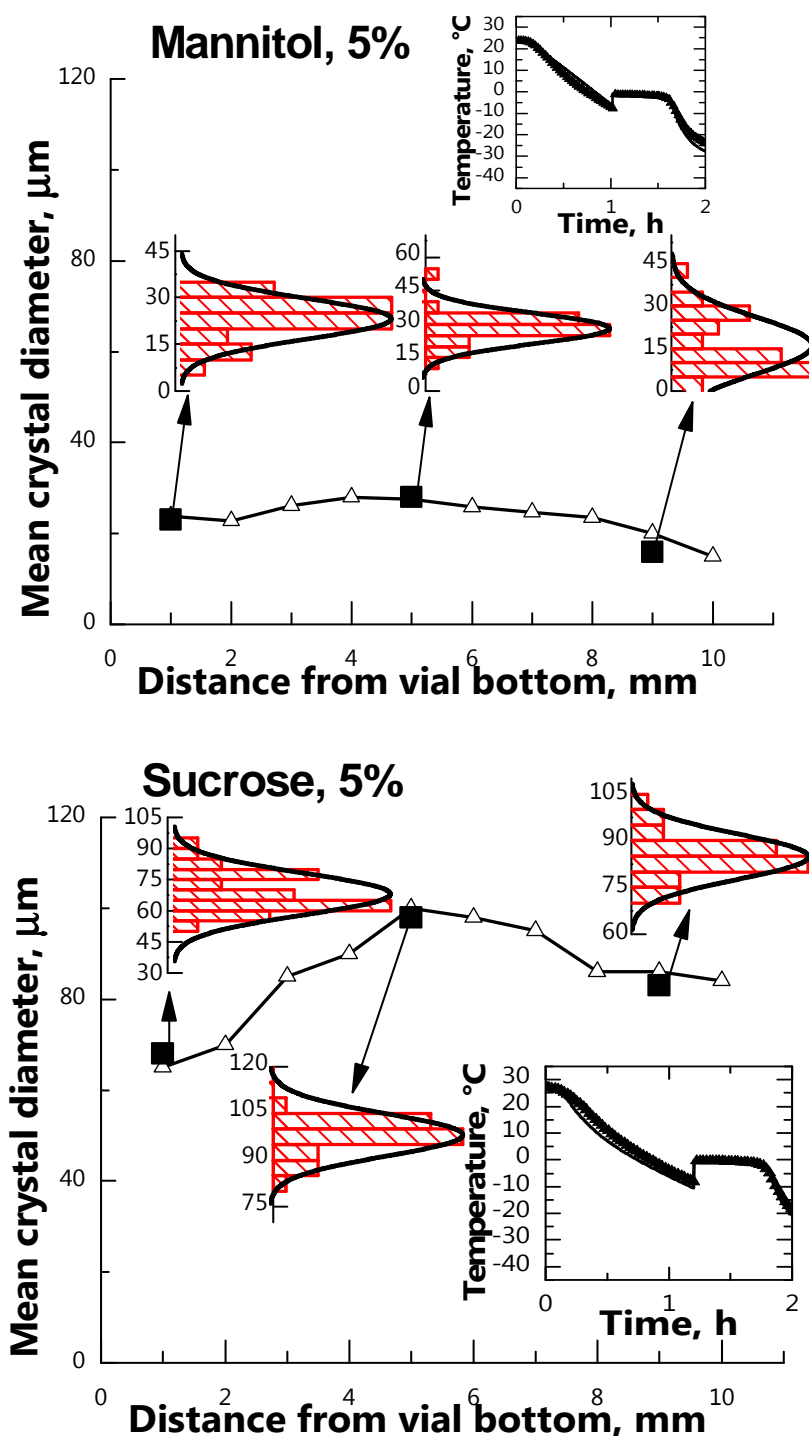


Fig. 4. Comparison between simplified model predictions ($-\Delta-$) and SEM observations (\blacksquare) for the average crystal size in the case of tests A and B (5% w/w mannitol or sucrose respectively). The histograms refer to the pore size radial distribution observed with SEM analysis. Insets show the temperature profiles at the product bottom as predicted by the model (solid black line) and as measured experimentally (black triangles).

The models were then tested for different operating conditions and concentration, but using mannitol as model solute. In particular, nucleation temperature, cooling rate and

concentration were changed. The product morphology, as measured using SEM analysis and as predicted by the model, was characterized using the crystal diameter averaged over the vertical direction. As can be seen in Table 4, the simplified model could predict with good accuracy the product morphology.

Table 4. Mean crystal size for tests A, C, D and E, as evaluated experimentally (Exp.) and by the simplified model (Sim. model)

	Mean crystal size, μm	
	Exp.	Sim. model
A	24	23
C	29	27
D	35	36
E	22	24

Tests A and C were performed using the same cooling rate, but the two samples had different nucleation temperatures. On the contrary, tests A and D had similar nucleation temperatures but were conducted using different cooling rates. As can be seen from the Table, the model could effectively predict the crystal size increase with increasing nucleation temperature (tests A and C), and with decreasing cooling rate (tests A and D). In fact, nucleation temperature and cooling rate are taken into account by the model in the v and θ terms.

Moreover, it is remarkable that the model worked fairly well even at the higher concentration of 10% w/w employed for test E. This means that the simplified model can be effectively applied to typical pharmaceutical formulations, whose concentration is generally smaller than 10% w/w.

Conclusions

In this paper, a model for the prediction of ice crystal size distribution in frozen products has been discussed. The model predictions have been validated upon experimental observations collected analysing with SEM microscopy the pore dimension of freeze-dried products. The validation has been performed for different operating conditions and concentrations, showing that the model developed can be efficiently applied to typical pharmaceutical solutions.

The dimension of ice crystals is a remarkable feature of products to be freeze-dried. For example, it strongly affects the duration of the primary and secondary drying phases, as well as the maximum temperature reached within the product. The model developed is therefore a solid starting point for a more conscious design of the freeze-drying process.

However, not all the problems have been solved. In the model developed there still is a term that must be evaluated from experimental data. Thus, further work is needed to make crystal size completely predictable from theoretical considerations, without need of experiments.

List of Symbols

a_s	empirical coefficient that accounts for the real ice crystals surface, -
b	coefficient that accounts for surface irregularities and crystal habit, $\text{K}^{2/3} \text{m}^{-2/3}$
D	vial base diameter, m
D_p	crystals diameter, m
h	heat transfer coefficient, $\text{W m}^{-2} \text{K}^{-1}$

ΔH_f	latent heat of crystallization, J kg ⁻¹
k_s	thermal conductivity of the solid, W m ⁻¹ K ⁻¹
m	mass of crystallized water, kg
n	number of discretization intervals, -
N	number of crystals, -
S_{ice}	surface of ice crystals, m ²
T	temperature, K
ΔT	temperature difference between air and product, K
t	time, s
Δt	time interval, s
V_{ice}	volume of ice crystals, m ³
z	axial coordinate, m
z_f	axial coordinate of the freezing front, m
Δz	axial interval, m
Δz_f	variation of the freezing front position, m

Greek letters

α	empirical coefficient of Equation 1, -
γ	solid-solid interfacial tension, J m ⁻²
ε	ratio between the volume of ice and the total volume of the system, -
θ	temperature gradient within the frozen zone, K m ⁻¹
λ_1	exponent of Equation 1, -
λ_2	exponent of Equation 1, -
v	freezing front velocity, m s ⁻¹
ρ_{ice}	density of ice, kg m ⁻³
τ	tortuosity, -

References

- [1] Franks, F., Auffret, T., *Freeze-Drying of Pharmaceuticals and Biopharmaceuticals*, RCS Publishing, Cambridge, UK (2007)
- [2] Rey, L., May, J., *Freeze-Drying/Lyophilization of Pharmaceuticals and Biological Products*, Marcel Dekker, Inc, New York, USA (2004)
- [3] Hottot, A., Vessot, S., Andrieu, J., *Freeze-drying of pharmaceuticals in vials: influence of freezing protocol and sample configuration on ice morphology and freeze-dried cake texture*, Chem. Eng. Process., **46**, (2006), 666-674
- [4] Bosca, S., Barresi, A., Fissore, D., *Design of a robust soft-sensor to monitor in-line a freeze-drying process*, Drying Technol., **33**, (2015), 1039-1050
- [5] Searles, J., Carpenter, J., Randolph, T., *The ice nucleation temperature determines the primary drying rate of lyophilization for samples frozen on a temperature-controlled shelf*, J. Pharm. Sci., **90**, (2001), 860-871
- [6] Bomben, J.L., King, C.J., *Heat and mass transport in the freezing of apple tissue*, J. Food Technol., **17**, (1982), 615-632
- [7] Kochs, M., Korber, C.H., Heschel, I., Nunner, B., *The influence of the freezing process on vapour transport during sublimation in vacuum freeze-drying*, Int. J. Heat Mass Transfer, **34**, (1991), 2395-2408
- [8] Kurz, W., Fisher, D.J., *Fundamentals of Solidification*, Trans Tech Publications, Switzerland (1992)
- [9] Nakagawa, K., Hottot, A., Vessot, S., Andrieu, J., *Modeling of freezing step during freeze-drying of drugs in vials*, AIChE J., **53**, (2007), 1362-1372